Tropical Journal of Pharmaceutical Research July 2022; 21 (7): 1355-1364
ISSN: 1596-5996 (print); 1596-9827 (electronic)

Available online at http://www.tjpr.org
http://dx.doi.org/10.4314/tjpr.v21i7.1

Original Research Article

Characterization, stability and solubility of co-amorphous systems of glibenclamide and L-arginine at different pH

Salma O Aragón-Aburto[1,2], Karina Mondragón-Vásquez[1], Gerardo Valerio-Alfaro[2], Jorge G Domínguez-Chávez[1]*

[1]Facultad de Bioanálisis Región Veracruz, Universidad Veracruzana, Agustín de Iturbide, 91700, [2]UNIDA, Tecnológico Nacional de México-IT Veracruz, Miguel A. de Quevedo 2779, 91860, Veracruz, México

For correspondence: **Email: jorgedominguez@uv.mx; **Tel:** +52 (228) 842 1700 ext. 26213*

Sent for review: 12 December 2021 *Revised accepted: 23 June 2022*

Abstract

Purpose: *To investigate the stability and solubility of co-amorphous systems of glibenclamide (GBC) with L-arginine (L-Arg) at different pH values.*
Methods: *Three co-amorphous solids of GBC and L-Arg were obtained by fast solvent evaporation using 2:1, 1:1 and 1:2 stoichiometries. All co-amorphous systems were characterized by XRPD, FTIR, RAMAN and NMR-solid state as well as thermal techniques such as DSC and TGA. The stability of co-amorphous systems was evaluated by indicative stability and stability in relevant physiological media was measured at different pH values.*
Results: *The chemical characterization suggest that there was no proton transference between L-Arg and GBC indicative of co-amorphous solids. Stability studies showed that all the co-amorphous solids are unstable under humid conditions and only the co-amorphous system of GBC: L-Arg 1:2 was stable in all the pH values tested. Solubility studies at different pH values showed that the co-amorphous GBC: L-Arg 1:1 and 1:2, showed increasing solubility values even at pH < 7 (0.6468 mg/mL at pH 1.2 for co-amorphous GBC: L-Arg 1:2 at the first hour) where free GBC was not soluble.*
Conclusion: *Co-amorphous systems of GBC and L-Arg, is an interesting strategy to increase the solubility of poorly-soluble drugs at acidic pH values*

Keywords: *Co-amorphous, Glibenclamide, L-Arginine, Solubility, Stability*

Tropical Journal of Pharmaceutical Research is indexed by Science Citation Index (SciSearch), Scopus, Web of Science, Chemical Abstracts, Embase, Index Copernicus, EBSCO, African Index Medicus, JournalSeek, Journal Citation Reports/Science Edition, Directory of Open Access Journals (DOAJ), African Journal Online, Bioline International, Open-J-Gate and Pharmacy Abstracts

INTRODUCTION

Pharmaceutical solids can be present in multiple forms (e.g., crystals, polymorphs, and others), which gives the opportunity to select the solid form that possess the most suitable physicochemical properties to ensure an effective therapeutic effect [1]. In this sense, the transformation of a crystalline drug into its amorphous form is a promising approach to improve the physicochemical properties of drugs [2]. Owing to the low packing efficiency and lack of large-range order, amorphous solids possess high molecular mobility and high potential energy relative to the crystalline forms [3]. This results in two of the most important properties that can impact the physicochemical properties such as solubility and bioavailability. Thus, amorphous

drugs, generally, are more soluble than their corresponding crystalline forms, making them attractive to the pharmaceutical industry [4]. In contrast, the high internal energy and enhanced molecular mobility in amorphous solids are also responsible for their higher chemical reactivity, high hygroscopicity and tendency to crystallize, which could occur during manufacturing, storage or administration. Consequently, the search for new methodologies that allow the stabilization of drugs in amorphous forms has become an interesting field of research [5]. Recently, the stabilization of amorphous drugs through the establishment of intermolecular interactions with small molecules (co-formers) that reduce the molecular mobility and increase the solubility of the drug has been reported to be responsible for giving rise to multicomponent amorphous systems (the so-called co-amorphous systems) [6]. Among the diverse co-formers used to obtain co-amorphous drugs are amino acids (like L-Arginine), which can establish strong interactions with the drug in the solid-state, generating a positive effect on amorphous solid formation and physical stability [7].

Glibenclamide (GBC) is a hypoglycemic drug class II according to the Biopharmaceutical Classification System that is poorly soluble. Its solubility depends strongly on the pH value of the test medium (< 0.004 mg/mL in acidic and neutral aqueous media and 0.02 mg/mL at pH > 7) [8]. This poor solubility translates to poor dissolution and unpredictable bioavailability [9]. On this basis, this research reports the characterization of three co-amorphous drugs of GBC: L-Arg in 2:1, 1:1 and 1:2 stoichiometries. Their biopharmaceutical properties, such as stability and solubility in relevant physiological media, were evaluated.

EXPERIMENTAL

Materials

Glibenclamide (GBC) and L-Arginine (L-Arg) were purchased from Sigma-Aldrich Co. (St. Louis, MO, USA). Solvents were purchased from local dealers and were used as received without further purification.

Preparation of amorphous GBC and co-amorphous material

The GBC amorphous and co-amorphous systems of GBC: L-Arg were prepared by fast solvent evaporation technique. One gram of GBC or the mixture of GBC: L-Arg in 2:1, 1:1 or 1:2 stoichiometries, were placed in a round bottom flask and dissolved completely in 100 mL of methanol. The mixtures were evaporated at 80 °C in a rotary evaporator under vacuum until a dry solid was formed. The resulting solid was scraped and placed in vials for further to analysis.

X-ray diffraction, spectroscopic and thermal characterizations

X-ray powder diffraction (XRPD) was performed using a Bruker D2 Phaser diffractometer (Bruker AXS GmbH, Germany) with Cu K_α radiation (λ = 1.541 Å). The FTIR spectra were analyzed using a Nicolet iS50 Thermo Scientific spectrograph (Thermo Electron Scientific Instruments LLC, Madison, Wisconsin USA) attached with a diamond crystal attenuated total reflectance. Confocal Raman spectra were collected using a confocal Raman microscope (Witec alpha 300R, WITec, Ulm, Germany), equipped with a CCD detector. Surface samples were excited using a 632 nm He-Ne laser. The SS-NMR spectra were recorded at room temperature on a 500 MHz Bruker Avance III HD instrument equipped with cross polarization (CP)/magic angle spinning (MAS) sequence pulse. The UV-Vis spectra were carried out on Scinco S-3100 spectrophotometer with diode array detector. Samples were analyzed in 1 cm quartz cells at 300 nm using the corresponding dissolution media in which the sample was dissolved. The DSC thermograms were obtained using a TA Instruments Q2000 DSC (TA-Instruments-Waters LLC, New Castle, Delaware, USA) equipped with a refrigerated cooling system (RCS-90), under nitrogen gas flow of 50 mL/min and using aluminum Tzero pans and sealed with no-hermetic Aluminum Tzero lids. Thermogravimetric analysis (TGA) were obtained using a TA Instruments Q50 TGA (TA-Instruments-Waters LLC, New Castle, Delaware, USA) under a nitrogen gas flow of 50 mL/min. The samples were heated at a heating rate of 20 °C/min starting from 30 to 400 °C. The mass loss percentage was calculated using TA-Universal analysis 2000 software (version 4.7A).

Biopharmaceutical characterization, solubility in relevant pH values

Buffer solutions employed in the experiment were: 0.05 M borate buffer (pH 9.5), 0.2 M phosphate buffer (pH 7.4), 0.2 M phosphate buffer (pH 6.8), 0.2 M acetate buffer (pH 4.5) and 0.2 M hydrochloric acid and potassium chloride buffer (pH 1.2). All the buffer solutions were prepared according to USP [10].

Calibration curves of GBC

Calibration curves were performed to determine

GBC concentrations in different solutions. Initially, a stock solution of GBC with a known concentration was prepared. Different samples were prepared by dilution of the stock solution and the new concentrations were calculated. The absorbance of all the samples prepared was obtained by UV-Vis spectroscopy at 300 nm and the obtained absorbance was plotted against concentration where the slope of the linear regression is the coefficient of absorptivity. All the experiments were carried out in triplicate and the average slope was obtained (ε_{300} = 2434.7 L/mol/cm for 0.05 M borate buffer, pH 9.5). The absorptivity coefficient could be calculated only in 0.05 M borate buffer, because GBC was not soluble in other buffer solutions.

Solubility studies

For each of the co-amorphous phase, a super-saturated solution was prepared using the respective buffer solution. The mixture was stirred at 37.5 °C for 24 h, whereupon 200 µL samples were taken at 1, 4, 8 and 24 h, and filtered through a 0.45 µm pore disk. An additional 20 µL was added to 2 mL of the respective medium and read into a UV–Vis spectrophotometer at a wavelength of 300 nm. The concentration was calculated from the absorbance and the Lambert–Beer equation using the same extinction coefficients previously calculated.

Indicative stability

The co-amorphous powders were stored at 40 and 50 °C with 0 % relative humidity (RH) and additionally at 40 °C 75 % RH condition for 1 month. After this period, the samples were analyzed by PXRD in order to detect diffraction peaks due to crystallization of GBC or L-Arg. All the studies were carried out in triplicates.

Stability in relevant physiological media

The stability of the co-amorphous phases was determined in all the physiological media previously indicated. About 80 mg of each sample was placed in a glass vial with two drops of the respective buffer and stirred at 37.5 °C. After 1 h a small amount (approximately 20 mg) was removed from the vial, dried at room temperature (24 °C), and analyzed by PXRD to detect diffraction peaks due to crystallization or changes in the IR spectra. This procedure was repeated every hour for a total of 5 h.

Statistical analysis

The measurements were in triplicates. Mean comparison between the solubility in the co-amorphous systems and the solubility in GBC crystalline and GBC amorphous states was carried out using one-way analysis of variance (ANOVA). Significant differences ($p < 0.05$) were determined by Tukey test. Statistical analysis was carried out using Origin Pro 2019 software (Origin Lab Corporation Northampton, MA 01060 USA).

RESULTS

X-ray diffraction

The corresponding XRPD diffractograms showed a diffuse “halo” scattering with absence of Bragg reflections that confirms the obtaining of amorphous phases in all cases.

FT-IR spectra

FT-IR spectra (Figure 1) showed a general reduction in the intensity of the bands and the loss of spectral resolution upon fast solvent evaporation amorphization; this is attributed to the inherently higher degree of molecular disorder associated with the amorphous forms. The most important bans for the amorphous GBC and the respective co-amorphous forms of GBC:L-Arg are two bands at 1625 and 1634 cm^{-1} for C=N stretch, two small shoulders at 1698 and 1683 cm^{-1} that could be attributed to the stretching vibration of urea carbonyl in GBC and the asymmetric bending vibration of the amine group in L-Arg, finally observed was the bending vibration of the guanidinium group at 1634 cm^{-1} and the asymmetrical and symmetrical stretching vibration of the COO^- bond at 1538 and 1400 cm^{-1}. For co-amorphous GBC: L-Arg 2:1 and 1:2, extra signals could be observed at 1705 and 1556 cm^{-1} assigned to the stretching carbonyl vibration of the second molecule of GBC and L-Arg respectively. Table 1 shows the selected signals for amorphous GBC and the three co-amorphous systems, these signals (also indicated in Figure 1).

Confocal Raman images

Confocal Raman microscopy experiments were performed to determine the homogeneity and purity of the 2:1, 1:1 and 1:2 GBC: L-Arg co-amorphous systems previously described. The Raman mappings obtained (Figure 2a, Figure 2b and Figure 2c), showed a homogeneous surface, with scattered black caused by laser defocusing during the data collection due to surface irregularities of the co-amorphous systems. The physical mixture of GBC: L-Arg in 1:1 stoichiometry (Figure 2d) showed two different

regions (indicated with the narrows), where the specific Raman spectra correlate with the Raman spectra reported in the literature for GBC (on top) and L-Arg (below).

SS-NMR spectra

The SS-NMR spectra for crystalline GBC, the co-amorphous systems and L-Arg as well as the full assignment and numeration used for GBC and L-Arg, are shown in Figure 3. The shift of the most important signals is show in Table 2. The spectra corresponding to the co-amorphous systems showed wide and poorly defined signals, confirming the high molecular disorder due to the increase in molecular orientations that occur when it is converted from the crystalline state to the amorphous state. The spectra of GBC: L-Arg 2:1 and 1:2 maintain a very similar signal patterns and shifts in comparison with the spectrum of GBC:L-Arg 1:1.

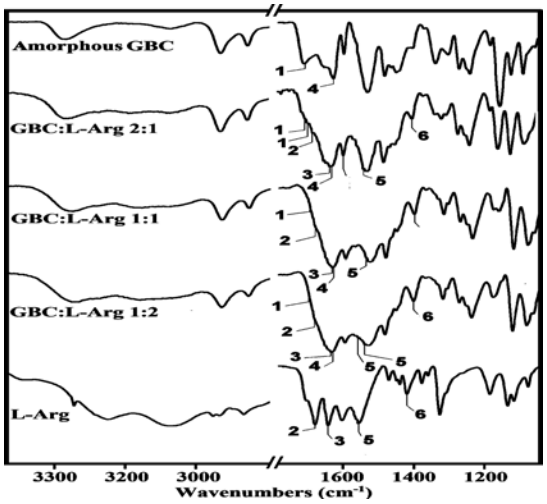

Figure 1: FTIR Spectra of amorphous GBC, L-Arg and the co-amorphous systems. The numbers are related to signals in Table 1. The region between 1800 and 2900 cm^{-1} was omitted for sake clarity

Table 1: Relevant bands displacement (in cm^{-1}) of the IR spectra amorphous GBC, L-Arg and the three co-amorphous systems previously obtained. **Key**: [a] as a little shoulder, [b] broad band, [c] merge in a broad band

	Tentative assignation	Amorphous GBC	L-Arg	GBC:L-Arg 2:1	GBC:L-Arg 1:1	GBC:L-Arg 1:2
1	v (C=O) stretch. Urea in GBC	1706	-	1705[ba], 1698[ba]	1698[ba]	1698[ba]
2	v (NH_2) asym. Bend. In L-Arg	-	1678	1683[ba]	1683[ba]	1683[ba]
3	v (N-H) bend. Guanidinium in L-Arg	-	1644	1634[cb]	1634[cb]	1634[cb]
4	v (C=N) stretch. Imidic acid in GBC	1625	-	1629[ac]	1629[ac]	1629[ac]
5	v (COO^-) asym. Stretch. In L-Arg	-	1556	1538	1538	1556[ac], 1538
6	v (COO^-) sym. Stretch. In L-Arg	-	1419	1400	1400	1400

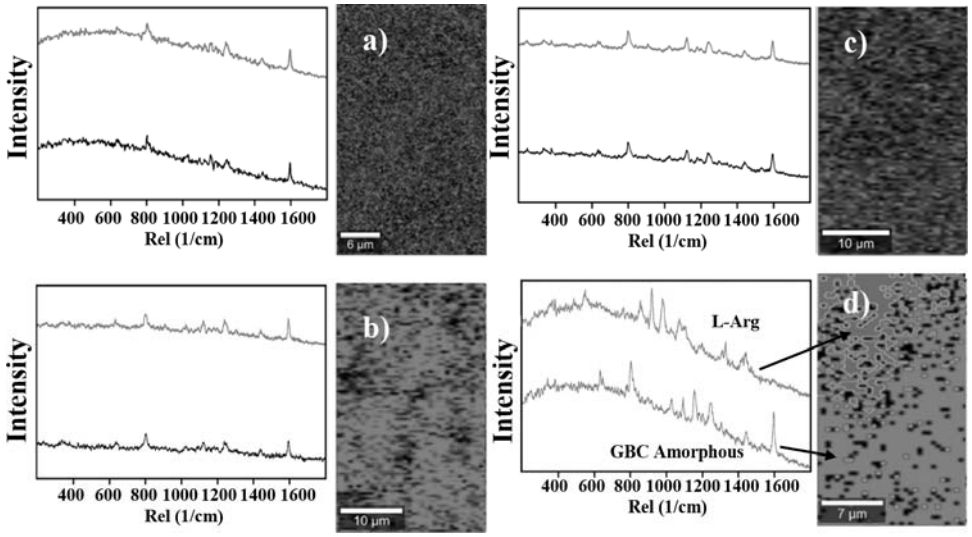

Figure 2: Raman mappings and associated Raman spectra of (a) GBC: L-Arg 2:1, (b) GBC:L-Arg 1:1, (c) GBC:L-Arg 1:2 and (d) Physical mixture of GBC and L-Arg in 1:1 stoichiometry

This helps to suppose that the GBC:L-Arg 2:1 and 1:2 maintain a solid structure similar to the co-amorphous GBC: L-Arg 1:1. However, in the spectrum of GBC: L-Arg 2:1, a small signal appears at 137.9 ppm which, in correlation with the signal at 138.6 ppm in amorphous GBC, was assigned to the *ipso* 1' carbon of the second GBC molecule, suggesting that GBC molecules contained in the co-amorphous system maintain a different pattern of molecular interaction as it was observed in the FT-IR spectrum.

DSC and TGA analysis

The DSC thermograms for the co-amorphous solids (Figure 4) was observed in the first heating. The DSC thermogram (shown in discontinuing lines) reveals an endothermic event between 85 and 91 °C, with a weight loss in TGA that correlates with a desolvation process of 0.5 mol of MeOH (Table 3). This confirms the preparation of solvated co-amorphous MeOH. After the desolvation process, a glass transition was observed at higher temperatures (87.69, 98.36 and 99.13 °C for GBC: L-Arg 2:1, 1:1 and 1:2, respectively). Finally, at further higher temperatures (T_{rc} = 149 - 167 °C), an exothermic event that correlates with a crystallization process of GBC was observed to immediately decompose as the temperature increases.

Stability

To determine the tendency toward recrystallization of the co-amorphous systems, an indicative stability study was performed. The diffractograms of co-amorphous solids stored at 40 and 50 °C in 0 % relative humidity (RH) maintained the characteristic diffuse halo of amorphous systems, and no diffraction peaks of the starting materials were detected.

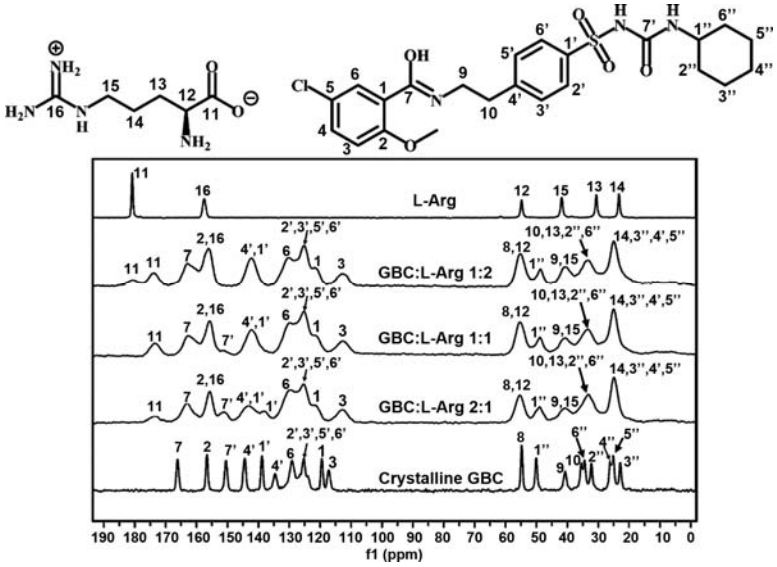

Figure 3: SS-NMR spectra and assignment of crystalline GBC, GBC: L-Arg 2:1, GBC:L-Arg 1:1, GBC:L-Arg 1:2 and L-Arg

Table 2: Principal signals in the SS-NMR spectra and their shift in ppm of GBC crystalline, GBC Amorphous, L-Arg and the three co-amorphous phases obtained. The carbon number correspond to numeration in Figure 3

Carbon No	GBC Crystalline	GBC Amorphous	GBC:L-Arg 2:1	GBC:L-Arg 1:1	GBC:L-Arg 1:2	L-Arg
7	166.2 (C=O)	163.7 (C=N)	163.4 (C=N)	163.3 (C=N)	163.2 (C=N)	-
1'	138.8	138.6	142.2 & 137.9	142.2	142.2	-
2'	125.3	126.2	125.2	125.2	125.2	-
3'	125.3	130.3	125.2	125.2	125.2	-
4'	144.4	145.2	143.2	142.2	142.2	-
5'	125.3	130.3	125.2	125.2	125.2	-
6'	125.3	126.2	125.2	125.2	125.2	-
7'	150.5	151.3	151.4[b]	152.0	overlap	-
11	-	-	173.6	173.6	173.6 & 180.7	180.0
12	-	-	55.3	55.3	55.2	54.8
16	-	-	155.7	155.7	156.0	157.5

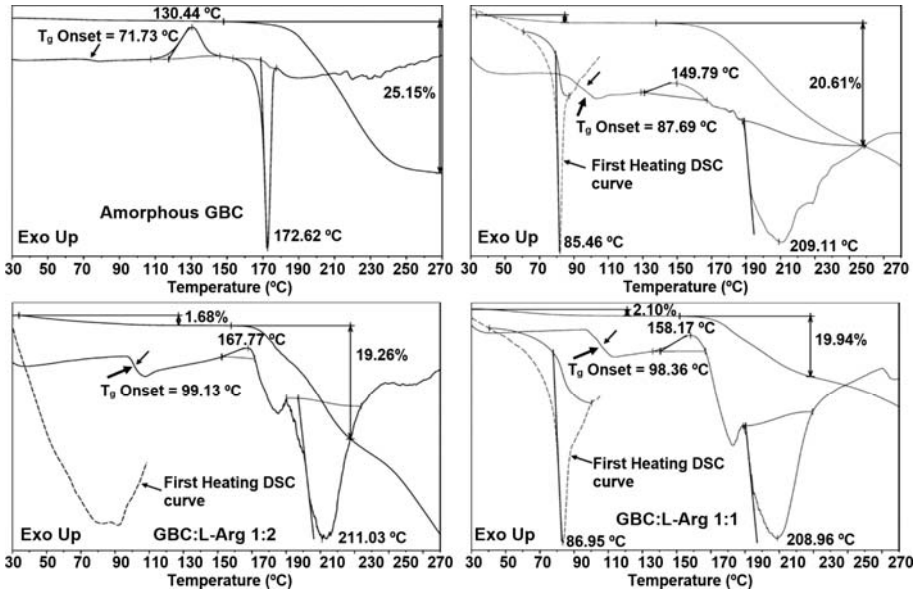

Figure 4: Thermal diagrams of DSC and TGA of GBC and the co-amorphous systems obtained

Table 3: Events and values observed in the DSC and TGA themograms. **Key**: N-CHF: N-ciclohexylformamide fragment in GBC. Decarbox: Decarboxylation of L-Arg

Compound	DSC events		TGA Events		
	Peak T (°C)	***Thermal Process***	***Onset Temp. (°C)***	***Assignment***	***% Weight loss (Exp./Cal.)***
Amorphous GBC	71.73	Glass Transition			
	130.44	Recrystallization			
	172.62	Decomposition	147.88	1 mol N-CHF	25.15/25.56
GBC:L-Arg 2:1	87.69	Glass Transition	35.32	Desolvation 0.5mol MeOH	1.28/1.36
	149.79	Recrystallization			
	209.11	Decomposition	143.76	2 mol N-CHF	20.61/21.16
GBC:L-Arg 1:1	98.36	Glass Transition	39.31	Desolvation 0.5mol MeOH	2.10/2.34
	158.17	Recrystallization			
	208.96	Decomposition	151.74	1 mol N-CHF	19.94/18.45
GBC:L-Arg 1:2	99.13	Glass Transition	33.85	Desolvation 0.5mol MeOH	1.68/1.86
	167.77	Recrystallization			
	213.52	Decomposition	158.05	1 mol N-CHF/Decarbox.	19.26/19.95

Also, no changes in the FTIR spectra were observed. However, when the co-amorphous systems were subjected to 40 °C and 75 % RH storage conditions, crystallization began, and diffraction peaks in their diffractograms corresponded to crystalline GBC. In the diffractograms obtained from the stability test in relevant physiological media for co-amorphous GBC: L-Arg 2:1 and GBC: L-Arg 1:1, peaks corresponding to crystalline GBC, at the first and fourth hours were observed, indicating that co-amorphous systems are not stable. However, the co-amorphous GBC: L-Arg 1:2 was completely stable for up to 24 h and at any pH-value.

Solubility

Figure 5 shows the solubility profiles for crystalline, amorphous and co-amorphous systems at 1, 4 and 8 h and different pH values. Crystalline GBC is slightly soluble at pH 9.5 while the solubility of amorphous GBC extends up to pH 7.8 and in pH 6.8, For co-amorphous GBC: L-Arg 2:1, the solubility values at pH 9.5 are very similar to amorphous GBC and without drastic changes in solubility during the experiment, however, the solubility of the co-amorphous 2:1 at pH 7.4 drastically decreases until it becomes insoluble.

The results of the solubility in the different pH values are presented in the Table 4. All the solubility values of the co-amorphous systems varied significantly ($p < 0.05$) with the solubility values of GBC crystalline and GBC amorphous.

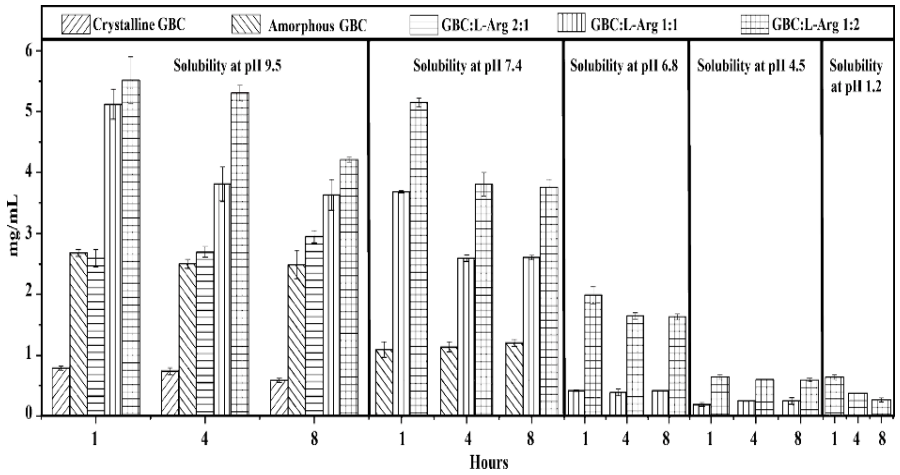

Figure 5: Solubility test of crystalline GBC, amorphous GBC and the co-amorphous phases at different times and physiological media

Table 4: Solubility values of GBC crystalline, GBC amorphous and all the co-amorphous systems at different pH values

pH-value	Hour	Crystalline GBC	Amorphous GBC	GBC:L-Arg 2:1	GBC:L-Arg 1:1	GBC:L-Arg 1:2
9.5	1	0.7915 ±0.034	2.6786 ±0.056	2.592 ±0.14	5.117 ±0.247	5.512 ±0.382
	4	0.738 ±0.054	2.498 ±0.071	2.692 ± 0.088	3.81 ±0.28	5.302 ±0.129
	8	0.5881±0.034	2.487 ±0.229	2.945 ± 0.1	3.63 ±0.25	4.211 ±0.04
7.4	1	Insoluble	1.072 ±0.124	Insoluble	3.6093 ±0.019	5.0443 ±0.073
	4	Insoluble	1.112 ±0.082	Insoluble	2.5432 ±0.049	3.7291 ±0.187
	8	Insoluble	1.1816 ±0.54	Insoluble	2.5536 ±0.034	3.683 ±0.1275
6.8	1	Insoluble	Insoluble	Insoluble	0.419 ±0.013	1.971 ±0.142
	4	Insoluble	Insoluble	Insoluble	0.391 ±0.054	1.632 ±0.053
	8	Insoluble	Insoluble	Insoluble	0.4205 ±0.002	1.618 ±0.047
4.5	1	Insoluble	Insoluble	Insoluble	0.1901 ±0.032	0.6304 ±0.038
	4	Insoluble	Insoluble	Insoluble	0.248 ±0.009	0.5888 ±0.005
	8	Insoluble	Insoluble	Insoluble	0.247 ±0.054	0.5854 ±0.027
1.2	1	Insoluble	Insoluble	Insoluble	Insoluble	0.6468 ±0.038
	4	Insoluble	Insoluble	Insoluble	Insoluble	0.3811 ±0.011
	8	Insoluble	Insoluble	Insoluble	Insoluble	0.2698 ±0.033

DISCUSSION

The principal goal in characterizing a pharmaceutical product that has undergone a co-amorphization process is to elucidate the nature of the molecular interaction to determine if the product is a real co-amorphous system or has been transformed into a salt. The general rule states that a component may donate a proton if the difference in pKa between the drug and the co-former is greater than 3. Experimental pKa for GBC is between 6 and 6.8 [13] and the pKa of the L-Arg amine is 9.0 [14] (since carboxylic acid protonates to the guanidinium group due to the large pKa difference), the theoretical limit of the transfer of the proton between GBC toward the L-Arg amine is set.

The formation of a salt between GBC and L-Arg would imply the loss of the nitrogen proton located between the carbonyl and sulfonyl functional groups of GBC and the protonation of the amino group of L-Arg to form a negative charge on the carbonyl oxygen in GBC and the formation of a $C\text{-}NH_3^+$ ion in L-Arg. These charged species would give rise to important changes in the FTIR, Raman and SS-NMR spectra. However, the respective spectra did not show important changes in the bands assigned for the stretching of the carbonyl group in GBC or the bending of NH_2 of L-Arg. For example, the Raman spectra showed (with little intensity) the $C\text{-}NH_2$ band and in SS-NMR spectra for the co-amorphous systems, the signal assigned to carbon 12 shows a slight shift ($\Delta\delta$ = 0.4-0.5 ppm), with respect to the signal observed in the L-Arg spectrum. This is consistent with the establishment of molecular interactions (hydrogen bridges) between GBC and L-Arg and is not large enough to be attributed to a possible proton transfer by GBC to L-Arg.

The FTIR, Raman and SS-NMR spectra of the GBC: L-Arg 2:1 and 1:2 co-amorphous systems are very similar to the spectra of GCB: L-Arg 1:1, and only extra bands or signals assigned to the second molecule are observed. This leads to the supposition that all co-amorphous solids maintain a basic molecular structure with a 1:1 stoichiometry. In the 2:1 and 1:2 ratios, the second molecule in excess seems to occlude into the amorphous structure. Based on the shifts and changes observed in the spectra, it can be concluded that the functional groups that seem to establish strong hydrogen bridges are the urea nitrogen in GBC and the carboxylate and guanidinium groups of L-Arg. Furthermore, the benzene sulfonyl ring shows considerable displacements in the SS-NMR spectrum, which could be attributed to the establishment of aromatic interactions with another GBC molecule.

The thermal analysis (DSC and TGA) in all co-amorphous solids show endothermic events with weight loss that correlates with a desolvation process of 0.5 mol of MeOH. This confirms the preparation of solvated co-amorphous MeOH in co-amorphous GBC:L-Arg 2:1 and 1:1. This event shows a sharp and well-defined peak that is indicative that MeOH could be a structural solvent, whereas in the 1:2 co-amorphous GBC:L-Arg, the desolvation process was observed as a wide and not well-defined band that could be indicative that MeOH was only occluded in the amorphous structure.

After the desolvation process, a single glass transition was observed at higher temperatures (87.69, 98.36 and 99.13 °C for GBC: L-Arg 2:1, 1:1 and 1:2, respectively) than the temperature observed for amorphous GBC (71.73 °C). This difference is important since an increase in the T_g value indicates that co-amorphous systems are more stable than amorphous GBCs thus indicating the formation of homogeneous phases. In this phase, drug interacts with the co-former through intermolecular interactions. Above the T_g temperature, the co-amorphous systems enter a rubbery state, and the molecular motion increases, which causes phase separation. At higher temperatures (T_{rc} = 149 - 167 °C), an exothermic event that correlates with a crystallization process of GBC was observed. The high temperature and the lower enthalpy in which this event occurs compared to amorphous GBC confirm the stability of the co-amorphous systems obtained. As shown in Figure 7, in the co-amorphous systems, a single glass transition (T_g) that indicates the formation of homogeneous phases can be observed, where the drug interacts with the co-former through intermolecular interactions [17].

The stability of the co-amorphous systems subjected to 40 and 50 °C without RH maintained was to be expected, since the maximum temperature that the co-amorphous systems were subjected to was below their T_g. At temperatures below the T_g, the molecular mobility responsible for crystallization decreased until crystallization was inhibited. However, humidity was present for crystallization to begin. This result suggests that the water absorption during the moisture-induced experiment causes the disruption of the molecular interactions in the co-amorphous system, while the plasticizing effect of water increases the molecular mobility in the co-amorphous solids and accelerates the amorphous phase separation. That is the origin of the nucleation and crystallization of the components in the co-amorphous solids.

The instability in relevant media of the co-amorphous 2:1 and 1:1 could be attributed to the interactions that arginine could establish with the GBC molecules, which are not strong enough to stabilize the co-amorphous phase, and induce phase separation and crystallization of GBC. However, the extra L-Arg molecule in the 1:2 co-amorphous systems could form extra intermolecular interactions that stabilize and prevent the crystallization of GBC even for up to 24 h.

The principal problem of GBC is its low solubility in physiological media. In this sense, the use of water-soluble amino acids, such as L-Arg, which could form stable co-amorphous systems, is an interesting strategy to modify the physicochemical properties of hydrophobic drugs such as GBC.

For all co-amorphous GBC: L-Arg, the solubility values at pH 9.5 were similar to the solubility values of amorphous GBC and without drastic changes in solubility during the experiment. This suggest that, as determined in the spectroscopic characterization, the second molecule of GBC does not establish very strong intermolecular interactions in the co-amorphous systems. In contact with the medium, this lack of strong intermolecular interactions could cause the immediate separation of the co-amorphous solids and induce precipitation and solubilization of the drug in free form. Unexpectedly, the solubility of the 2:1 co-amorphous system at pH 7.4 drastically decreases. This could be attributed to the fact that once the co-amorphous phase is separated and since the pH does not favor drug resolubilization, the drug begins to crystallize in the solution, thereby becoming insoluble. This

observation is supported by the analysis of the stability in relevant media, where the presence of diffraction peaks of crystalline GBC in the diffractograms at the first hour showed the crystallization of GBC.

For the GBC: L-Arg 1:1 and 1:2 co-amorphous solids, the solubility at pH 9.5 and 7.4 showed a significant increase regarding crystalline and amorphous GBC at the first hour. At 4 and 8 h, a slight decrease in solubility was observed, possibly attributed to a "parachute effect" of the co-amorphous systems. Solubility studies at pH values of 6.8, 4.5, and 1.2, where crystalline and amorphous GBCs were completely insoluble, show that at pH 6.8, the solubility of the 1:2 co-amorphous system was good (1.91 mg/mL) at the first hour and remains practically unchanged for up to 8 hours. In contrast, the solubility of the 1:1 co-amorphous system had a drastic decrease, dissolving only 0.4 mg/mL during the first hour and maintaining the same concentration until 8 h are completed. At pH 4.5, the solubility of both co-amorphous systems decreased considerably, showing concentration values at the first hour of 0.1901 and 0.6304 mg/mL, respectively, and maintaining practically the same solubility after 4 and 8 h. At pH 1.2, GBC: L-Arg 1:2 presented a similar solubility (0.6468 mg/mL) in the first hour to the solubility obtained at pH 4.5 at 4 and 8 hours; the solubility of the co-amorphous systems decreased slightly until reaching a solubility of 0.2698 mg/mL.

Based on the results obtained, it can be inferred that the increase in solubility and solubilization at low pH values of the 1:1 and 1:2 co-amorphous systems concerning crystalline and amorphous GBC seems to depend on two factors. The first factor could be attributed to the stoichiometry in which L-Arg was found in co-amorphous systems. In this sense, Maity and coworkers reported that, in the case of proteins, their solubility increased when arginine was found in high concentrations due to the formation of intermolecular interactions with proteins [19]. This was the reason why the 1:2 co-amorphous system had the greatest increase in solubility. The extra L-arginine molecule could establish, in solution, new intermolecular interactions forming a much more stable complex. This formation of the more stable complex was supported by co-amorphous 1:2 GBC: L-Arg being the only stable co-amorphous system at the different pH values studied. The second factor involved (and that could explain the solubility that the 1:2 co-amorphous system dipping at pH 1.2) the change in ionization of arginine. At that pH, arginine is doubly protonated with the guanidinium and ammonium fragments, while the carboxylic acid maintains its proton. This arginine structure could stabilize the complex formed at pH 1.2, preventing it from precipitating/crystallizing in the medium.

CONCLUSION

Based on the results obtained in this study, GBC: LArg 1:2 co-amorphous system shows higher solubility, even at acidic pH-values, than the original drug. Therefore, obtaining co-amorphous systems could be an interesting strategy to modify the physicochemical properties of drugs without modifying their chemical structure.

DECLARATIONS

Acknowledgements

This work was supported by Consejo Veracruzano de Investigación Científica y Desarrollo Tecnológico (COVEICyDET) through project number: 15 1008/2021. Also, we thank to Laboratorios Senosian S.A. de C.V. for indicative stability studies and Dr. Hugo Morales Rojas for CP-Mass SS-NMR spectra.

Funding

None provided.

Ethical approval

None provided.

Availability of data and materials

The datasets used and/or analyzed during the current study are available from the corresponding author on reasonable request.

Conflicts of interest

No conflict of interest is associated with this work

Contributions of authors

We declare that this work was done by the authors named in this article and all liabilities pertaining to claims relating to the content of this article will be borne by the authors. Aragón-Aburto collected and analyzed all the data, Mondragón-Vásquez and Domínguez-Chávez conceived and designed the study and wrote the manuscript, Valerio-Alfaro reviewed the manuscript for publication. All authors read and approved the manuscript for publication.

REFERENCES

1. *Byrn SR, Zografi G, Chen XS. Solid-state properties of pharmaceutical materials. New Delhi: John Wiley & Sons, 2017; p 1.*
2. *Löbmann K, Grohganz H, Laitinen R, Strachan C, Rades T. Amino acids as co-amorphous stabilizers for poorly water-soluble drugs – part 1: preparation, stability and dissolution enhancement. Eur J Pharm Biopharm 2013; 85(3): 873-881.*
3. *Babu NJ, Nangia A. Solubility advantage of amorphous drugs and pharmaceutical cocrystals. Cryst Growth Des 2011; 11(7): 2662-2679.*
4. *Schittny A, Huwyler J, Puchkov M. Mechanisms of increased bioavailability through amorphous solid dispersions: A review. Drug Deliv 2020; 27(1): 110-127.*
5. *Laitinen R, Löbmann K, Strachan CJ, Grohganz H, Rades T. Emerging trends in the stabilization of amorphous drugs. Int J Pharm 2013; 453(1): 65-79.*
6. *Löbmann K, Laitinen R, Grohganz H, Gordon KC, Strachan C, Rades T. Co-amorphous drug systems: enhanced physical stability and dissolution rate of indomethacin and naproxen. Mol Pharm 2011; 8(5): 1919-1928.*
7. *Huang Y, Zhang Q, Wang JR, Lin KL, Mei X. Amino acids as co-amorphous excipients for tackling the poor aqueous solubility of valsartan. Pharm Dev Technol 2017; 22; 69-76.*
8. *Brockmeier D, Grigoleit HG, Leonhardt H. Absorption of glibenclamide from different sites of the gastro-intestinal Tract. Eur J Clin Pharmacol 1985; 29(2): 193-197.*
9. *Dastmalchi S, Garjani A, Maleki N, Sheikhee G, Baghchevan V, Jafari-Azd P, Valizadeh H, Barzegar-Jalali M. Enhancing dissolution, serum concentrations and hypoglycemic effect of glibenclamide using solvent deposition technique. J Pharm Pharm Sci 2005; 8: 175-181.*
10. *The United States Pharmacopeia. National Formulary 36. Vol. 1. Rockville (MD: United State Pharmacopeial Convention; 2018. Test Solutions; p. 5676.*
11. *Huang Y, Zhang Q, Wang JR, Lin KL, Mei X. Amino acids as co-amorphous excipients for tackling the poor aqueous solubility of valsartan. Pharm Dev Technol 2017; 22(1): 69-76.*
12. *Allu S, Suresh K, Bolla G, Chaitanya Mannava MK, Nangia A. Role of hydrogen bonding in cocrystals and co-amorphous solids: indapamide as a case study. CrystEngComm 2019; 21: 2043-2048.*
13. *Masereel B, Lebrun P, Dogné JM, de Tulio P, Pirotte B, Pochet L, Diouf O, Delarge J. First Synthesis of 4-Substituted Benzene sulfonyl cyanoguanidines. Tetrahedron Lett 1996; 37(40): 7253-7254.*
14. *Haynes WM (Editor). CRC Handbook of Chemistry and Physics, 97th Edn. Boca Raton: CRC press. 2017. p. 7-11.*
15. *Zografi G, Newman A. Introduction to amorphous solid dispersions. In Newman, Ann, editors. Pharmaceutical sciences encyclopedia: Drug discovery, development, and manufacturing. New Jersey: John Wiley & Sons; 2015. p.1-4.*
16. *Lehmann MS, Verbist JJ, Hamilton WC, Koetzle TF. Precision neutron diffraction structure determination of protein and nucleic acid components. Part V. Crystal and molecular structure of the amino-acid L-arginine dihydrate. J Chem Soc, Perkin 2 1973; 2: 133-13.*
17. *Nielsen LH, Rades T, Müllertz A. Stabilization of amorphous furosemide increases the oral drug bioavailability in rats. Int J Pharm 2015; 490(1-2): 334-340.*
18. *Maity H, Karkaria C, Davagnino J. Effects of pH and Arginine on the Solubility and Stability of a Therapeutic Protein (Fibroblast Growth Factor 20): Relationship between Solubility and Stability. Curr Pharm Biotechnol 2009; 10(6): 609-625.*